




Green synthesized selenium nanoparticles for ovarian cancer cell apoptosis

Hamed Amiri¹ · Seyed Isaac Hashemy^{1,2} · Zahra Sabouri³ · Hossein Javid⁴ · Majid Darroudi^{5,6} 

Received: 11 December 2020 / Accepted: 27 February 2021 / Published online: 17 March 2021
© The Author(s), under exclusive licence to Springer Nature B.V. 2021

Abstract

Over recent years, selenium nanoparticles (Se-NP) have been widely applied in nanomedicine science due to their exceptional physicochemical and biological properties. The available reports regarding the fabrication methods of these nanoparticles include several physical and chemical processes that are toxic, costly and non-environmentally. In this work, Se-NPs were synthesized through a rapid, biocompatible, safe, cost-effective and green chemistry approach that require the usage of bioactive compounds of honey. In addition, the obtained nanoparticles were characterized by UV–Vis, XRD, TEM, FESEM, EDX and FTIR analysis. The in vitro anticancer efficiency of biosynthesized Se-NPs@Honey was also examined on A2780 ovarian cancer cells, which interestingly exhibited a concentration-dependent anti-proliferative activity toward human ovarian cancer cells with the IC₅₀ value of 60.95 µg/mL. Furthermore, their apoptotic effects were confirmed through the means of flow cytometry analysis that was performed by an annexin V–FITC kit and the assessment of apoptosis gene expression. According to the gathered data, Se-NPs@Honey can promote oxidative damage through the generation of reactive oxygen species in A2780 cells as well. Therefore, our findings strongly suggest that green synthesized Se-NPs by the usage of honey could stand as an efficient anticancer agent in the future.

Keywords Selenium nanoparticles · Green synthesis · Honey · Apoptosis · Anticancer

✉ Seyed Isaac Hashemy
Hashemyi@mums.ac.ir

✉ Majid Darroudi
darroudim@mums.ac.ir; majiddarroudi@gmail.com

Extended author information available on the last page of the article

Introduction

Nanotechnology concentrates on the design, synthesis, characterization and application of nanoscale materials and devices throughout the various medical sciences. This branch of knowledge has an enormous potential to advance the therapeutic strategies of biomedical and biotechnology researches, as well as clinical diagnosis and treatments [1, 2]. There are a variety of nanoscale tools and structures in nanomedicine including nanomatching, nanofibers, nanocomposite and quantum dots [3–5]. Inorganic nanoparticles are known as one of the most significant nanostructures, likely considered as a diagnostic marker, that can distinguish various diseases especially cancers [6–8]. Nanoparticles contain a large number of biological applications due to their unique physicochemical properties containing small size, large surface area-to-mass ratio and biocompatibility [9]. Selenium is categorized as an essential element in minerals since a small portion of it is required to be taken daily as a dietary supplement for health maintenance [8]. Additionally, this element is a crucial component of enzymatic proteins in the form of selenocysteine that had been reported to contain antioxidant properties [10, 11]. Apparently, selenoenzymes are able to protect human tissues and organs against oxidative damages [11]. Clinical and preclinical studies have indicated that this micronutrient plays a major role in the functionality of immune system, as well as in preventing neurodegenerative diseases and cancers [12, 13]. Nowadays, researchers have proposed that Se-NPs can stand as a suitable replacement for Se in biomedical studies due to their unique physicochemical features and biological activities. In comparison with the other forms of this element, Se-NPs contain certain significant advantages such as low toxicity, biocompatibility and surface modification [14, 15]. Numerous *in vitro* and *in vivo* studies have indicated that Se-NPs possess multiple beneficial pharmacological effects including anti-inflammatory, antioxidant, antimicrobial and anticancer activities [16, 17]. In addition, the protective effects of Se-NPs against metal and drug-induced toxicity such as cisplatin, chromium, anastrozole and cadmium chloride have been well documented [18]. Moreover, Se-NPs have attracted the attention of many, especially in the field of cancer, since a notable number of studies have been suggestive of these nanoparticles potential for preventing and treating various tumors [14, 19]. The anticancer effects of Se-NPs mainly depend on shape, particle size, concentration and coated materials. Meanwhile, several studies have reported the remarkable ability of Se-NPs to elicit cytotoxicity against cancer cells through the various molecular and cellular mechanisms involving cell cycle arrest, oxidative stress, impairing mitochondria, DNA damage and induction of apoptosis [20, 21]. For instance, Dongxiao Cui et al. demonstrated that Se-NPs could strongly inhibit the *in vitro* proliferation of liver cancer cells through an apoptotic cell death mechanism [22]. In another study, ferulic acid-coated Se-NPs (FA-Se-NPs) are reported to induce apoptosis in HepG-2 cancer cells by increasing intracellular ROS generation and activating caspase-3/9 [23]. Additionally, there are several lines of evidences that have exhibited the capability of Se-NPs as a leading agent for the development of therapeutic strategies against various tumors [24,

25]. On the other hand, the unique surface properties of Se-NPs have given them the capability of loading therapeutic molecules, such as DNA, RNA, proteins and synthetic drugs, and made them suitable as the genes or drug carriers [18, 26]. Despite the fact that nanoparticles could be synthesized through a variety of physical and chemical techniques, the application of these procedures has decreased due to their limitations and disadvantages [27]. Some of the most important factors among these limitations include the high costs of essential hazardous chemical, as well as the long time intervals that are required to conduct their procedures [28]. Nowadays, these synthesizing techniques have been majorly replaced with "green chemistry" methods that involve the utilization of harmless and natural compounds instead of raw chemical materials [29–31]. The main sources of nanoparticle biological synthesis are biopolymers, certain types of food and plant extracts [32, 33]. As it is known, green synthesizing procedures can produce nanoparticles in different sizes and shapes, which leads to a variety of physicochemical and biological properties [34]. Relatively, the green synthesis of Se-NPs has particularly attracted a lot of interest since this method can increase the efficiency of their qualities. Consistently, several studies have suggested biological synthesizing procedures for Se-NPs that involve the usage of *Allium sativum* and other particular microorganisms [35, 36]. In addition, a recent study had successfully synthesized Se-NPs through the usage of gelatin as a reducing agent and therefore obtained nanoparticles with remarkable anti-bacterial features [37]. Honey stands as a valuable nutrient and suitable candidate among the food sources that are exerted for nanoparticle green synthesis since it has exhibited its exceptional pharmacological, physical and chemical properties in traditional medicines [38]. Next to its significant functionality in preventing and ameliorating the treatment of many diseases, this nutrient contains a wide variety of substances including different amino acids, proteins, vitamins and sugars. Due to the existence of monosaccharides (fructose and glucose) and polyphenolic compounds (hesperetin, kaempferol, ellagic acid, etc.) in its chemical composition, honey could be applied as a reducer throughout the synthesizing processes and also function as a stabilizing agent for controlling the size of nanoparticle [39, 40]. Ovarian cancer is one of the most common malignancies in women that lead to the largest number of deaths in comparison with the other types of female reproductive cancers [41]. Similar to other cases of cancers, the efficacy of current treatments has been decreased due to the occurrence of drug resistance. Therefore, new therapeutic strategies such as nanotechnology and the application of nanoparticles combined with chemotherapeutic agents are required to develop a promising therapeutic target for reducing the rate of tumor growth in many types of cancer [42]. In this regard, the aim of this study was set to introduce an easy, low-cost and novel biosynthetic method for producing selenium nanoparticles that require the usage of natural honey for the first time, which were also characterized in terms of size, morphology and spectral properties. Furthermore, the in vitro anticancer potential of Se-NPs@Honey were investigated against human ovarian cancer (A2780) cells based on their ability to induce apoptotic cell death.

Materials and method

Cell culture

Human epithelial ovarian carcinoma cell line A2780 was purchased from Pasteur Institute of Iran (Tehran, Iran). To begin the process, cells were incubated in the conditions of 37 °C, 5% CO₂ and 95% humidity within the culture medium RPMI1640 that was supplemented with 1% penicillin/streptomycin and 10% FBS. All of the involved experiments included the utilization of cells that were in the logarithmic phase of growth ($0.5\text{--}1.0 \times 10^6$ cells/mL).

Preparation of Se-NPs@Honey

Se-NPs@Honey were synthesized in this work through the chemical reduction of sodium selenite salt (Na₂SeO₃) that involved the usage of honey as a reducing and stabilizing agent. Initially, 50 mL of sodium selenite solution (10 mM) was prepared, and then, 10 mL of high-purity honey was diluted in 15 mL of distilled water. Thereafter, the mixture that contained honey was gradually added to sodium selenite solution for the purpose of controlling the nanoparticle size and polydispersity. The mixture solution was stirred at 60 °C for 24 h to synthesize the colloidal Se-NPs@Honey [43]. The occurrence of a gradual change in the color of final mixture, which was altered from colorless toward red, indicated the successful synthesis of Se-NPs@Honey. Subsequent to completing the reaction, the synthesized nanoparticles were centrifuged to be washed with distilled water and ethanol in a high-speed centrifuge (12,000 rpm) over several times. To conclude the process, Se-NPs@Honey were dried overnight at 80 °C to be evaluated for further analysis. The schematic green synthesis of Se-NPs@Honey is presented in Fig. 1.

Resazurin assay

The cell metabolic activity of Se-NPs@Honey was evaluated utilizing resazurin-based cytotoxicity assay. Resazurin assay is based on the capability of living cells to reduce Resazurin (non-fluorescent) to resorufin and dihydro-resorufin (highly fluorescent). Briefly, 2×10^4 cells were seeded in triplicates into 96-well plates. After administration of cells with various concentration of Se-NPs@Honey (3.9,

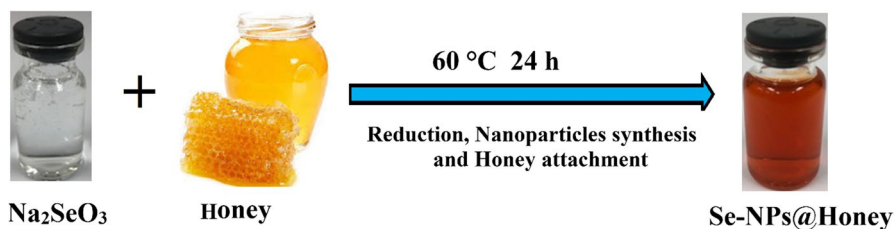


Fig. 1 Schematic plan of the green synthesis of Se-NPs@Honey

7.81, 15.62, 31.25, 62.5, 125, 250 and 500 $\mu\text{g}/\text{mL}$), the cells were incubated with 5% CO_2 at 37 °C for 24 and 48 h. The production of fluorescent dye (pink) was measured with PerkinElmer atomic absorption spectrophotometer at 600 nm and 570 nm, respectively. The metabolic activity of Se-NPs@Honey was determined through IC_{50} values, which was calculated with dose–response curve in GraphPad Prism[®] 6 software.

Measurement of reactive oxygen species

Effects of Se-NPs@Honey on the intracellular ROS level were tested by 2', 7'-dichlorodihydro fluorescein diacetate (DCFDA, Sigma, USA). Briefly, after 24 h incubation, A2780 cells were incubated for 30 min at 37 °C with 20 μM DCFDA. Next, cells were administered via various concentrations of Se-NPs@Honey (3.9, 7.81, 15.62, 31.25 and 62.5 $\mu\text{g}/\text{mL}$). Additionally, the tert-butyl hydro peroxide (TBHP) was used as a positive control for ROS generation. Ultimately, the relative fluorescence intensity of the 96-well plate was determined at 490/530 (Excitation/Emission) in PerkinElmer spectrophotometer.

Apoptosis/necrosis detection

Evaluation of apoptosis/necrosis by flow cytometry is performed by means of annexin-V and propidium iodide (PI) staining assay. Briefly, next of treatment (24 h), A2780 cells were washed with PBS and incubated with 100 μL of staining buffer including 2 μL of annexin-V–FITC for 30 min in the dark. Afterward, the number of stained cells was assessed through flow cytometer. It should be noted that the FITC–annexin V-positive and PI-negative are identified as early apoptosis and annexin-V-positive and PI-positive stained cells are representative of late apoptosis.

Gene expression assessment by quantitative real-time PCR (qRT-PCR)

The RNA extraction done from 60×10^4 cells after treatment with various concentrations of Se-NPs@Honey utilizing total RNA extraction mini kit (Parstous, Mashhad, Iran), according to manufacturer's guidelines. The total RNA quantity was measured by NanoDrop spectrophotometer (NanoDrop 1000TM, USA). Next, 1500 ngr of RNA was used to generate the complementary DNA (cDNA) by cDNA Synthesis Kit (Parstous, Mashhad, Iran). Subsequently, for qRT-PCR, the synthesized cDNA was mixed with SYBR Green (Ampliqon, Denmark) and specific primers including p53, Bax, Bcl-2 and survivin (pishgaman Co, Tehran, Iran). All amplifications were accomplished in Roche real-time thermal cycler, and glyceraldehyde-3-phosphate dehydrogenase (GAPDH) was measured as a housekeeping gene. Finally, the relative gene expression was calculated with the $2(-\Delta\Delta\text{Ct})$ method ($2^{-\Delta\Delta\text{Ct}}$).

Statistical analysis

All data are exhibited as the mean values \pm standard deviation of three independent experiments. Statistical analyses were specified with ANOVA followed by the Bonferroni's t-test for multi-group assessments. All analyses were exhibited using the GraphPad Prism[®] 6.0 software for Windows, and a significance level of $p < 0.05$ was adopted.

Results and discussion

Characterization

The UV–Vis spectrophotometry (CE-9500, Cecil, UK) technique was selected to identify the Se-NPs@Honey, and for this purpose, the relative absorption of colloidal solution was read at 200–800 nm. In addition, the shape and size of obtained nanoparticles were assessed by means of transmission electron microscopy (TEM, Philips Holland Tecnai-20). Accordingly, the colloidal solution of Se-NPs@Honey was put under ultrasonic irradiation for 30 min to acquire a homogeneous solution. Thereafter, a single drop of the sample was placed on copper grids to have the image of nanoparticles observed and evaluated. It should be noted that the suitable voltage and resolution of the experiment was set at 200 kV and the point of 0.27 nm, respectively. The X-ray diffraction pattern (XRD, Philips Co., Holland) was utilized to determine the phase and crystal structure of synthesized Se-NPs@Honey. In addition, we performed field emission scanning electron microscopy (FESEM, TESCAN BRNO-Mira3 LMU) to distinguish the morphology of these nanoparticles. The FESEM micrographs, which were obtained by the usage of energy-dispersive X-ray spectroscopy (EDX), provided detailed images of the nanopowders that were prepared for performing a further evaluation on the shapes of the sample. Finally, the Fourier transform infrared (FTIR, Shimadzu 8400, Japan) spectra of honey and Se-NPs@Honey were acquired to identify the functional groups that were bound distinctively on the biosynthesized Se-NPs.

Biosynthesis of Se-NPs@Honey

In order to perform a successful synthesis and obtain stable Se-NPs@Honey in the present work, honey was applied to function as a reducing and capping agent under facile conditions. According to Fig. 1, the biosynthesis of Se-NPs@Honey was first confirmed by observing a gradual change in the color of reaction medium that contained Na_2SeO_3 and honey within 24 h. Considering how the presence of red color is caused as the surface plasmon resonance of Se-NPs@Honey is excited, it can be indicated the selenium ions had successfully converted into selenium nanoparticles [44]. It is stated in the report of Hamed A. Ghramh et al. that fructose, glucose,

sucrose and proteins are the main ingredients of honey that can act as reducing agents and produce metallic nanoparticles [45].

UV-Vis Spectroscopy

The formation of Se-NPs through the usage of honey was further confirmed by recording the absorption spectra of Se-NPs@Honey colloidal solution in the range of 200–800 nm. The gathered data on UV-Vis spectra and band gap energy (E_g) plot of Se-NPs@Honey are exhibited in Fig. 2a, b. A sharp optical absorbance band detected at around 283 nm was indicative of the synthesis of well-dispersed Se-NPs (Fig. 2a). Moreover, the observed characteristic peak may be assigned to the surface plasmon resonance (SPR) band of Se-NPs@Honey [46], which is in agreement with the findings of D, Cui et al.[14]. The band gap energy (E_g) of these nanoparticles was obtained by evaluating the UV-Vis spectra data, which were calculated to be

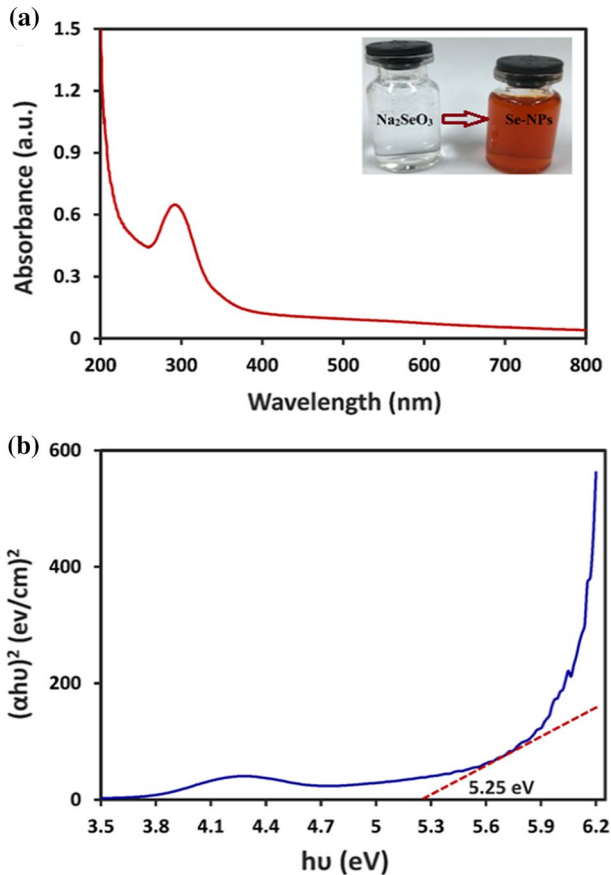


Fig. 2 UV-Vis spectrum (a) and estimated band gap of synthesized Se-NPs@Honey (b)

about 5.25 eV (Fig. 2b). It is interesting that the band gap energy of nanoparticles was observed to be higher than that of the bulk Se (1.74 eV).

XRD Pattern

The crystalline structure and phase determination of biosynthesized Se-NPs@Honey was assessed through the application of XRD analysis, which is displayed in Fig. 3. The results obtained from XRD pattern were confirmed via the Joint Committee on Powder Diffraction Standards (JCPDS file no # 06–362) [47]. The XRD pattern approved the amorphous nature of Se-NPs@Honey that were synthesized by honey due to the appearance of a broader peak while lacking any sharp Bragg reflections. Also, there had not been any peaks corresponding to other constituents throughout this pattern, which reflects the purity of these nanoparticles. The detection of an amorphous structure from the Se-NPs@Honey could be possibly explained by the capping of several functional groups of honey that were present on the surface of particles [48]. This result was in accordance with earlier studies that had been carried out on the green synthesis of Se-NPs by exerting the fruit extracts of *Emblica officinalis* [49], *Withania somnifera* leaves extract [50] and *Pseudomonas aeruginosa* [51]. Moreover, it has been proposed by some previous reports related to phase determination that stable amorphous Se-NPs are capable of displaying a better solubility and bioavailability throughout biological applications [52].

FESEM/PSA image

The presented FESEM/PSA images of Se-NPs@Honey in Fig. 4a, b confirm the uniform and spherical shape of the obtained nanoparticles (Fig. 4a). Moreover, an average diameter of around 57.7 nm was observed throughout the particle size distribution curve (Fig. 4b).

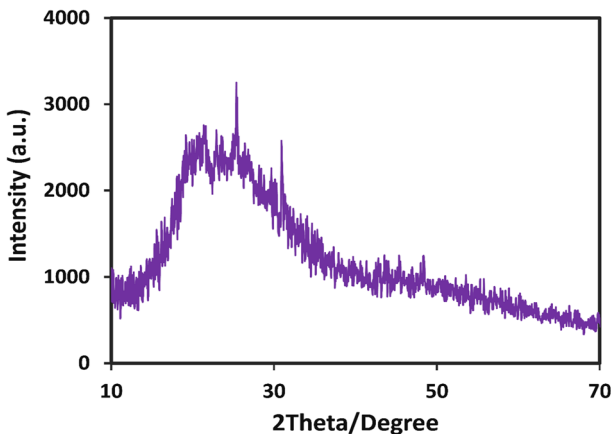


Fig. 3 XRD pattern of the biosynthesized Se-NPs@Honey

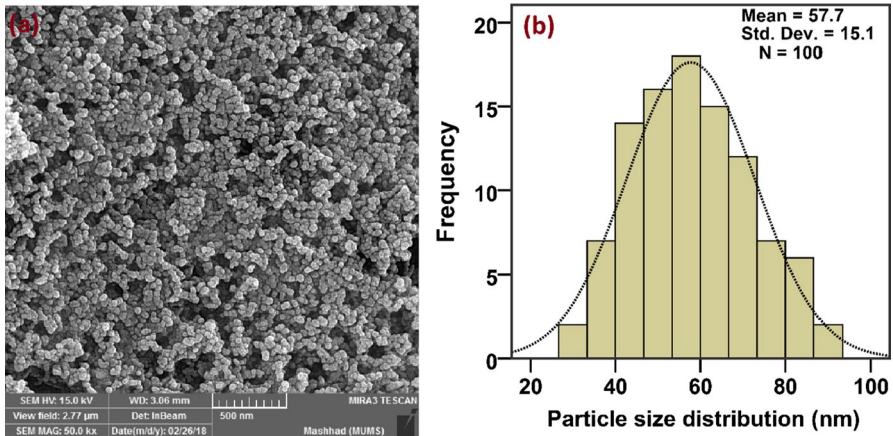


Fig. 4 FESEM image (a) and size distribution (b) of Se-NPs@Honey obtained under optimal conditions

EDX Analyze

The EDX technique was employed for determining the quantity and quality of Se-NPs@Honey, along with the elements that were present throughout the reaction mixture that were apparently involved throughout the production of nanoparticles. The result of this elemental microanalysis is illustrated in the form of a diagram in Fig. 5, which exhibits a completely distinct and intense peak that proves the presence of selenium element in the tested sample. The prominent spectral peak at around 1.38 keV supports the formation of Se element with high purity [53]. Also,

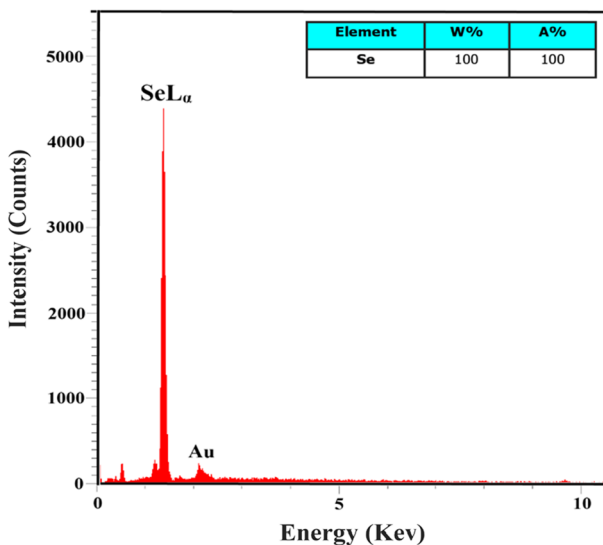


Fig. 5 EDX spectra of the synthesized Se-NPs@Honey

the performed elemental analysis presented the existence of gold at about 2.3 keV, which was applied in grid coating procedure.

TEM/PSA image

The TEM/PSA images of Se-NPs@Honey are displayed in Fig. 6a, b, which were employed to investigate their size, morphology and distribution [54]. The spherical shape of Se-NPs@Honey could be observed in the provided image, and according to PSA analysis, their average size was reported to be about 56 nm, which is very close to the results of FESEM image.

FTIR Analysis

The main ingredients in honey are mostly natural sugars (glucose, fructose and sucrose), minerals, proteins, polyphenols and vitamins. FTIR measurement was used to determine the available functional groups involved in the processes of bioreduction of sodium selenite and stabilization of the obtained Se-NPs@Honey. The FTIR spectra of the honey and the synthesized Se-NPs@Honey are shown in Fig. 7. Based on the IR spectra, the strong and elongated absorption band at 3368 cm^{-1} might be related to the hydroxyl group ($-\text{OH}$), indicating the presence of phenols or flavonoids as the main reducing agents in the chemical composition of honey for the synthesis of nanoparticles [55]. Also, the band observed at around 2920 cm^{-1} can be associated with the C–H stretching vibrations of aromatic compounds [56]. Besides, two peaks have found in the range of 1661 and 1057 cm^{-1} , which may be attributed to the C=O stretch of primary amines and C–O bending vibrations of protein in honey, respectively [57]. The current results of the FTIR spectroscopy study demonstrated that honey has the ability to perform both functions of reduction

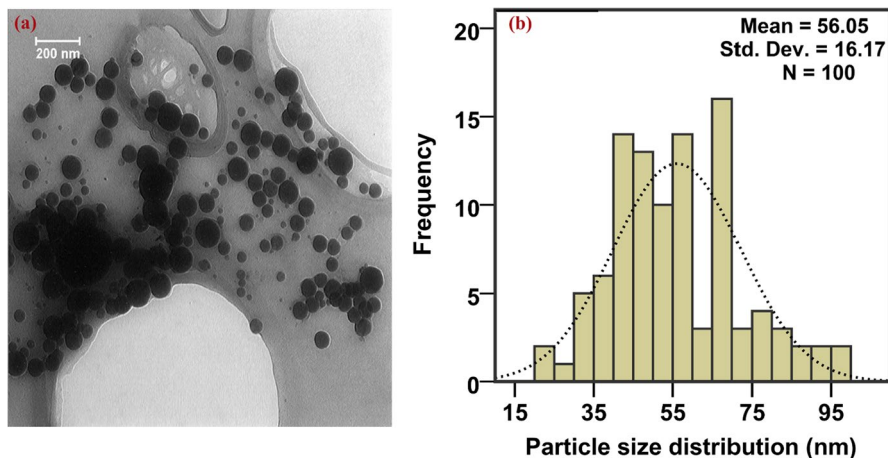


Fig. 6 TEM micrograph (a) and particles size distribution (b) of Se-NPs@Honey

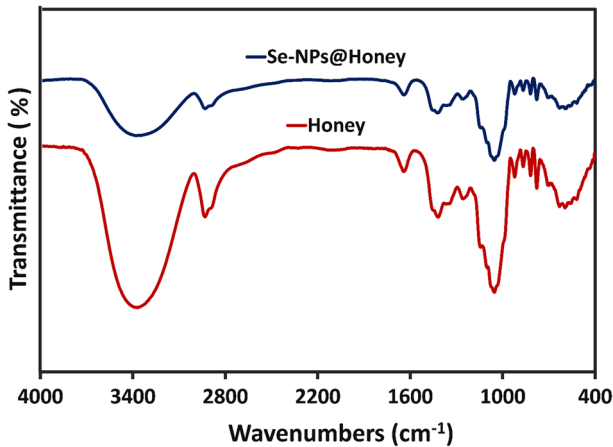


Fig. 7 FTIR spectra of the honey and the synthesized Se-NPs@Honey

and stabilization for the biosynthesis of Se-NPs. Likewise, the slight change in the intensity and position of the peaks in the spectrum of Se-NPs@Honey indicates the involvement of honey biomolecules in the process of formation and stabilization of nanoparticles. Previous studies have indicated that the nanoparticles can bind to various functional groups in the honey (i.e., phenol, alcohol, amides and protein) [58]. According to H. Haiza et al. [59], it has been also reported that proteins in honey can bind to nanoparticles and make them stable through carboxylate ions as well as free amino groups of the amino acid residues.

Se-NPs@Honey inhibited proliferation of cancer cells

The *in vitro* anticancer potential of Se-NPs@Honey was evaluated at various concentrations (3.9, 7.81, 15.62, 31.25, 62.5, 125, 250 and 500 $\mu\text{g/mL}$) on human ovarian carcinoma A2780 cells through the employment of resazurin reduction assay. According to the exhibited cell viability results in Fig. 8, Se-NPs@Honey have clearly displayed anti-proliferative activity against A2780 cells with an IC_{50} at around 60.95 and 34.85 $\mu\text{g/mL}$ after 24 and 48 h of treatment, respectively, while no cytotoxicity was detected from honey alone treatment. It can be indicated from obtained outcomes, Se-NPs@Honey dose- and time-dependently decreased the survival of A2780 cells. Previous research studies have reported that Se-NPs are able to penetrate into various types of cells through different endocytosis pathways [60] and cause toxic effects. Although the toxicity mechanism of selenium nanoparticles against tumor cells is not fully comprehended yet, some *in vitro* observations suggest that the intracellular accumulation of Se-NPs@Honey can eventually lead to cell death through different ways including causing damage to cell components, inhibition of angiogenesis, cell cycle arrest and activation of apoptotic pathways [61]. It is well known that the cellular uptake of nanoparticles is a crucial factor in their cytotoxicity against cells [62]. Relatively in this study, the biomolecules of honey that take part in the formation and stability of selenium nanoparticles can

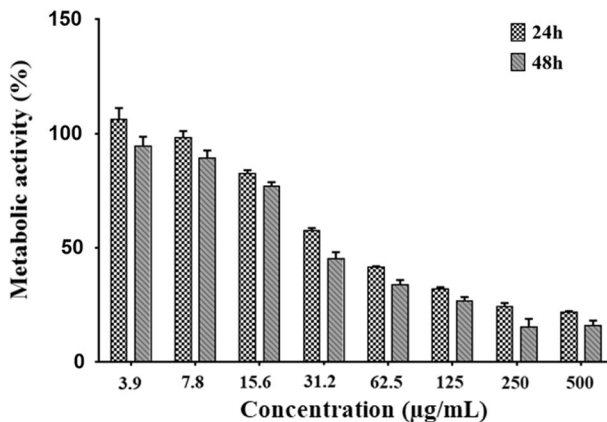


Fig. 8 Cytotoxicity effect of Se-NPs@Honey on A2780 cell survival using resazurin assay

easily enter cancer cells, which consequently enhances their cell internalization and anticancer efficacy of nanoparticles [63]. Due to the significant toxicity of Se-NPs@Honey against human cancer cells, the following experiments were carried out to further evaluate the anticancer effects of these nanoparticles.

Effect of Se-NPs@Honey on reactive oxygen species in tumor cells

Over-production of ROS under conditions of oxidative stress is considered as a major cause of cell components dysfunction, which can eventually lead to induction of cell death [64]. It has been indicated by numerous studies that the usage of many anticancer drugs leads to the activation of apoptosis-related cellular signaling pathways through increased cellular ROS levels [65]. Moreover, various papers have reported that certain nanoparticles, including metal and metal oxide nanoparticles, can induce programmed cell death by increasing the production of ROS [66, 67]. Relatively, in order to investigate the association of induced cell death with oxidative stress, we have measured the levels of ROS in the A2780 cells that had been treated with Se-NPs@Honey by the application of DCFH-DA assay [68]. As depicted in Fig. 9, once the A2780 cells had been treated with various concentration (62.5, 31.25, 15.62, 7.81, and 3.9 µg/mL) of Se-NPs@Honey for 24 h, the generation of ROS in ovarian cancer cells has been considerably increased in a concentration-dependent manner in comparison with the control group. The ROS elevation in cancer cells has been observed to be in 15.6, 31.2, and 62.5 concentrations of Se-NPs@Honey, and the maximum of DCF fluorescence intensity was detected at the IC₅₀ value. It is indicated by these results that the participation of intracellular ROS may have the critical role throughout the Se-NPs@Honey-induced cancer cell death, which is consistent with the findings of previous studies. According to the observations of Hengyang Li et al., there has been an elevation in the ROS generation of cervical cancer (HeLa) cells that had been exposed to Se-NPs [69]. In addition, they have also reported that the synthesized nano-selenium by ferulic acid has provoked

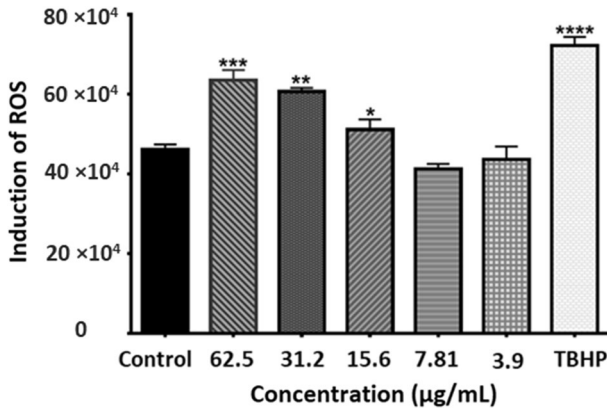


Fig. 9 Se-NPs@Honey-induced formation of reactive oxygen species in A2780 cells

apoptosis in HepG-2 cells through ROS production. Considering observed results, it can be suggested that the anticancer activity of selenium NPs may be highly related to generation of ROS.

Se-NPs@Honey induces apoptosis in A2780 cell line

Apoptosis is known as a specific type of cell death and a regulated process that occurs under certain conditions [70]. According to the recorded observations of numerous reports, many nanoparticles exhibit their anticancer activities through the activation of various signaling pathways (mainly including p53 activation, caspase-dependent and Bcl-2 down-regulation/BAX up-regulation), which can eventually lead to cellular apoptosis [71]. To quantitatively detect the apoptosis that had been induced by Se-NPs@Honey in ovarian cancer cells, we have applied a flow cytometric analysis based on annexin V–FITC/PI double staining assay in order to estimate the rates of cell apoptosis. Annexin V conjugated with FITC (fluorescent dye) binds in a high-specificity manner to the cell membrane of phosphatidylserine, which is translocated to the extracellular membrane in the course of early apoptosis. It should be considered that propidium iodide (or PI) is a DNA-binding dye and can be applied to stain DNA content in late apoptotic/necrotic cells where the plasma membrane has been wholly compromised [72]. Therefore, the combined usage of both fluorescent agents can facilitate the required differentiation among early apoptotic cells (annexin V-positive/PI-negative), late apoptotic cells (annexin V/PI-double-positive), necrotic cells (annexin V-negative/PI-positive) and living cells (annexin V/PI-double-negative) [14]. In this study, we have performed the process of dual staining after having A2780 cells exposed to different concentrations (3.9, 7.81, 15.6, 31.2, and 62.5 µg/mL) of Se-NPs@Honey for 24 h. As demonstrated in Fig. 10, 98.7% of untreated cancer cells have been viable (double-negative cells), whereas the rate of total apoptosis (annexin-V and annexin-V/PI-dual-positive) in groups that had been treated with Se-NPs@Honey at concentrations of 31.2 and 62.5 µg/mL has been significantly increased. Overall, the findings of flow cytometric have revealed

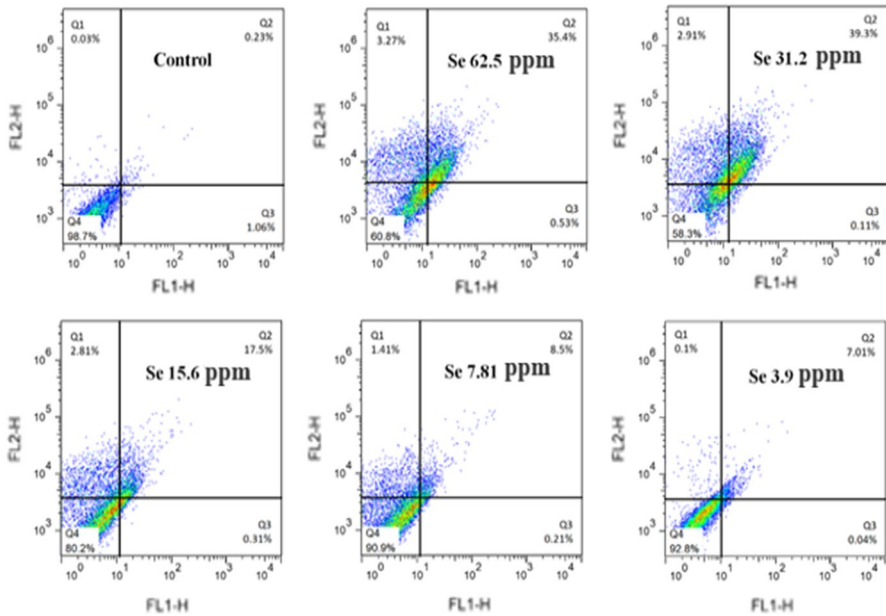


Fig. 10 The rates of annexin-V/PI-double-positive and annexin-V cells were drastically increased as compared to untreated control cells

that the toxicity effect of biosynthesized Se-NPs@Honey on human ovarian cancer cells could be mainly related to the stimulation of apoptotic pathways rather than necrotic process. It is notable that similar results to our observations have been recently reported, which states that selenium nanoparticles can induce cell apoptosis. It has been demonstrated in the work of Y Li et al. that Se-NPs synthesized by Galangin have remarkably promoted the apoptosis pathway in HepG2 cells via the production of ROS and activation of caspase-3, AKT and p38 signaling pathways [73]. Similarly, Xiong Gao et al. have reported that Se-NPs are capable of inducing apoptosis in HT29 and Hela cells as well [74].

Effect of Se-NPs@Honey treatment on gene expression

To further study the pro-apoptotic effects of Se-NPs@Honey on A2780 cells, we have performed the quantitative analysis of apoptosis-related genes (p53, Bcl-2, Bax and C-myc) through the application of quantitative real-time PCR. As exhibited in Fig. 11, the exposure of Se-NPs@Honey to A2780 cancer cells has altered the expression of mentioned genes and according to the obtained results, the mRNA expression of p53 (tumor suppressor gene) and Bax (pro-apoptotic gene) in ovarian cancer cells has been up-regulated in comparison with the control group. However, in contrast to this observation, the mRNA expression of Bcl-2 (anti-apoptotic gene) and C-myc has displayed a down-regulated behavior in Se-NPs@Honey-treated cells. The recorded gene expression alterations of our study have once again

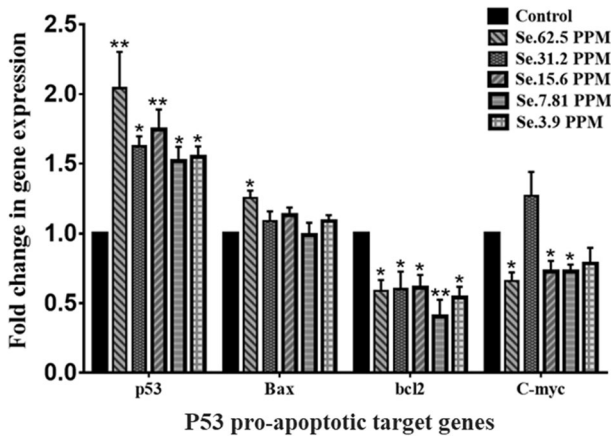


Fig. 11 Comparison of p53, Bax, Bcl-2 and C-myc mRNA levels in the A2780 cells after 24 h of treatment with Se-NPs@Honey

approved the fact that the cytotoxicity effect of Se-NPs@Honey in ovarian cancer cells is processed through the induction of apoptotic pathway. P53 gene is known to be the most famous tumor suppressor that contains a crucial functionality throughout carcinogenesis inhibition via cell cycle arrest, anti-angiogenic effect, senescence and chiefly promote apoptosis [75]. Accordingly, it can be contemplated that p53 pathway is able to stand as a significant target for designing anticancer drugs. It has been also suggested in previous studies that the assessment of Bax/Bcl-2 gene ratio can be employed to determine the susceptibility of cancer cells toward apoptosis [76]. In 2016, the work of Maqusood Ahamed et al. has reported that Cobalt iron oxide nanoparticles can induce cell death in human liver cancer (HepG2) cells causing a considerable enhancement in the gene ratio of Bax/Bcl-2 expression [66]. C-myc is known as a regulatory gene factor that can adjust the activity of a large number of genes that are involved in cell division, while its over-expression can lead to the inducement of uncontrolled cell proliferation [77]. Recently, certain nanoparticles have been modified and synthesized that had become capable of effectively preventing the growth of cancer cells by reducing the C-myc expression. A study of Abdulwahab Ali Abuderman et al. has reported that silver nanoparticles (Ag-NPs) can inhibit the activity of C-myc in human liver carcinoma cells and lead to the occurrence of cell cycle arrest [78].

Conclusion

In the current paper, Se-NPs@Honey were successfully synthesized by the usage of honey through a facile, cost-effectiveness and eco-friendly manner that lacked the involvement of any hazardous chemicals. Honey was selected to function as both reducing and capping/stabilizing agents for the formation of nanoparticles. Microscopic analysis of Se-NPs@Honey showed that the average particle size was about

57 nm and spherical in shape. In addition, according to the gathered data, Se-NPs@Honey are capable of exhibiting a significant cytotoxic activity against A2780 ovarian cancer cells in a dose- and time-dependent manner. The treatment with Se-NPs@Honey also led to an up-regulation in the gene expression of p53, Bax (pro-apoptotic factors) and down-regulation in the gene expression of Bcl-2 and C-myc. Furthermore, Se-NPs@Honey markedly increased the production of intracellular ROS. Consequently, the anticancer activity of Se-NPs@Honey may be strongly associated with the oxidative stress and induction of apoptosis. Taken all together, the current findings demonstrate that the use of honey as a good natural source for biosynthesis of Se-NPs could be useful for the development of green synthesis routes, and this study also suggests that Se-NPs@Honey may be applied as an effective anticancer agent without side effects to treat various cancers, especially ovarian cancer in the future. However, further preclinical (animal) studies are required to fully elucidate the mechanisms of anticancer activity of Se-NPs@Honey on cancer cells.

Acknowledgements The technical support for this work has been provided by Mashhad University of Medical Sciences (Grant # 970802) based on the MSc thesis of Mr. H. Amiri.

Declarations

Conflict of interest The authors declare that they have no conflict of interest.

References


1. E. Nourmohammadi, H. Khoshdel-sarkarizi, R. Nedaenia, H.R. Sadeghnia, L. Hasanzadeh, M. Darroudi, R.K. Oskuee, *J. Cell. Physiol.* **234**, 4 (2019)
2. M. Guo, Y. Li, Z. Lin, M. Zhao, M. Xiao, C. Wang, T. Xu, Y. Xia, B. Zhu, *RSC Adv.* **7**, 83 (2017)
3. S. Kargozar, M. Mozafari, *Mater. Today: Proc.* **5**, 7 (2018)
4. Y. Chang, L. He, Z. Li, L. Zeng, Z. Song, P. Li, L. Chan, Y. You, X.-F. Yu, P.K. Chu, *ACS Nano* **11**, 5 (2017)
5. Z. Chen, Z. Chen, A. Zhang, J. Hu, X. Wang, Z. Yang, *Biomater. Sci.* **4**, 6 (2016)
6. F. Wang, C. Li, J. Cheng, Z. Yuan, *Int. J. Environ. Res. Public Health* **13**, 12 (2016)
7. K. McNamara, S.A. Tofail, *Adv. Phys.: X* **2**, 1 (2017)
8. S. Skalickova, V. Milosavljevic, K. Cihalova, P. Horoky, L. Richtera, V. Adam, *Nutrition* **33**, 83 (2017)
9. I. Khan, K. Saeed, I. Khan, *Arab. J. Chem.* **12**, 7 (2019)
10. E. Zoidis, I. Seremelis, N. Kontopoulos, G.P. Danezis, *Antioxidants* **7**, 5 (2018)
11. H. Steinbrenner, B. Speckmann, L.-O. Klotz, *Arch. Biochem. Biophys.* **595**, 113 (2016)
12. Z. Sun, Z. Xu, D. Wang, H. Yao, S. Li, *Metallomics* **10**, 5 (2018)
13. J. Aaseth, J. Alexander, G. Björklund, K. Hestad, P. Dusek, P.M. Roos, U. Alehagen, *Biomaterials* **29**, 5 (2016)
14. D. Cui, T. Liang, L. Sun, L. Meng, C. Yang, L. Wang, T. Liang, Q. Li, *Pharm. Biol.* **56**, 1 (2018)
15. K. Kokila, N. Elavarasan, V. Sujatha, *New J. Chem.* **41**, 15 (2017)
16. V. Nayak, K.R. Singh, A.K. Singh, R.P. Singh, *New J. Chem.* **45**, 2849 (2021)
17. V. Nayak, K.R.B. Singh, A.K. Singh, R.P. Singh, *New J. Chem.* (2021). <https://doi.org/10.1039/D0NJ05884J>
18. A. Khurana, S. Tekula, M.A. Saifi, P. Venkatesh, C. Godugu, *Biomed. Pharmacother.* **111**, 802 (2019)
19. S.A. Wadhvani, M. Gorain, P. Banerjee, U.U. Shedbalkar, R. Singh, G.C. Kundu, B.A. Chopade, *Int. J. Nanomed.* **12**, 6841 (2017)
20. B. Yu, Y. Zhang, W. Zheng, C. Fan, T. Chen, *Inorg. Chem.* **51**, 16 (2012)

21. G. Zhao, X. Wu, P. Chen, L. Zhang, C.S. Yang, J. Zhang, *Free Radic. Biol. Med.* **126**, 55 (2018)
22. D. Cui, J. Ma, T. Liang, L. Sun, L. Meng, T. Liang, Q. Li, *Int. J. Boil. Macromol.* **137**, 829 (2019)
23. D. Cui, C. Yan, J. Miao, X. Zhang, J. Chen, L. Sun, L. Meng, T. Liang, Q. Li, *Mater. Sci. Eng.: C* **90**, 104 (2018)
24. G. Huang, Z. Liu, L. He, K.-H. Luk, S.-T. Cheung, K.-H. Wong, T. Chen, *Biomater. Sci.* **6**, 9 (2018)
25. B. Yu, T. Liu, Y. Du, Z. Luo, W. Zheng, T. Chen, *Coll. Surf. B: Biointerfaces* **139**, 180 (2016)
26. F. Maiyo, M. Singh, *Nanomedicine* **12**, 9 (2017)
27. M. Rafique, I. Sadaf, M.S. Rafique, M.B. Tahir, *Artif. Cells Nanomed. Biotechnol.* **45**, 7 (2017)
28. T. Abdelghany, A.M. Al-Rajhi, M.A. Al Abboud, M. Alawlaqi, A.G. Magdah, E.A. Helmy, A.S. Mabrouk, *BioNanoScience* **8**, 1 (2018)
29. M. Darroudi, M. Bagherpour, H.A. Hosseini, M. Ebrahimi, *Ceram. Int.* **42**, 3 (2016)
30. K. Kalishwaralal, S. Jayabharathi, K. Sundar, A. Muthukumaran, *Artif. Cells, Nanomed., Biotechnol.* **44**, 2 (2016)
31. E. Nourmohammadi, R.K. Oskuee, L. Hasanzadeh, M. Mohajeri, A. Hashemzadeh, M. Rezayi, M. Darroudi, *Ceram. Int.* **44**, 16 (2018)
32. M.E.T. Yazdi, J. Khara, H.R. Sadeghnia, S.E. Bahabadi, M. Darroudi, *Res. Chem. Intermed.* **44**, 2 (2018)
33. Z. Sabouri, A. Akbari, H.A. Hosseini, M. Darroudi, *J. Mol. Struct.* **1173**, 931 (2018)
34. S. Shoeibi, P. Mozdziaik, A. Golkar-Narenji, *Top. Curr. Chem.* **375**, 6 (2017)
35. P.B. Ezhuthupurakkal, L.R. Polaki, A. Suyavarana, A. Subastri, V. Sujatha, C. Thirunavukkarasu, *Mater. Sci. Eng.: C* **74**, 597 (2017)
36. S. Shoeibi, M. Mashreghi, *J. Trace Elem. Med. Biol.* **39**, 135 (2017)
37. M. Kazemi, A. Akbari, S. Soleimanpour, N. Feizi, M. Darroudi, *J. Cluster Sci.* **30**, 3 (2019)
38. N.A. Ismail, K. Shamel, M.M.-T. Wong, S.-Y. Teow, J. Chew, S.N.A.M. Sukri, *Mater. Sci. Eng.: C* **104**, 109899 (2019)
39. H.A. Ghramh, E.H. Ibrahim, M. Kilany, *Food Sci. Nutr.* **8**, 1 (2020)
40. S. Khorrani, F.J. Najafabadi, A. Zarepour, A. Zarrabi, *BioNanoScience* **9**, 3 (2019)
41. Y.-J. Choi, J.-H. Park, J.W. Han, E. Kim, O. Jae-Wook, S.Y. Lee, J.-H. Kim, S. Gurunathan, *Int. J. Mol. Sci.* **17**, 12 (2016)
42. B. Gidwani, A. Vyas, *Artif. Cells, Nanomed., Biotechnol.* **43**, 4 (2015)
43. M. Kazemi, A. Akbari, H. Zarrinfar, S. Soleimanpour, Z. Sabouri, M. Khatami, M. Darroudi, *J. Inorg. Organomet. Polym. Mater.* **30**, 8 (2020)
44. F.M. Mosallam, G.S. El-Sayyad, R.M. Fathy, A.I. El-Batal, *Microb. Pathog.* **122**, 108 (2018)
45. H.A. Ghramh, E.H. Ibrahim, M. Kilany, *Food Sci. Nutr.* **8**, 445 (2019)
46. K. Anu, G. Singaravelu, K. Murugan, G. Benelli, *J. Cluster Sci.* **28**, 1 (2017)
47. C. Dwivedi, C.P. Shah, K. Singh, M. Kumar, P.N. Bajaj, *J. Nanotechnol.* **2011**, 1 (2011)
48. J.-K. Yan, W.-Y. Qiu, Y.-Y. Wang, W.-H. Wang, Y. Yang, H.-N. Zhang, *Carbohydr. Polym.* **179**, 19 (2018)
49. L. Gunti, R.S. Dass and N.K. Kalagatur, *Frontiers in microbiology* **10**, (2019)
50. V. Alagesan, S. Venugopal, *Bionanoscience* **9**, 1 (2019)
51. A.J. Kora, L. Rastogi, *J. Environ. Manag.* **181**, 231 (2016)
52. S. Cavalu, E. Kamel, V. Laslo, L. Fritea, T. Costea, I.V. Antoniac, E. Vasile, A. Antoniac, A. Semencescu, A. Mohan, *Rev. Chim.* **68**, 12 (2017)
53. S.S. Salem, M.M. Fouda, A. Fouda, M.A. Awad, E.M. Al-Olayan, A.A. Allam, T.I. Shaheen, *J. Clust. Sci.* **32**, 1 (2020)
54. H. Forootanfar, M. Adeli-Sardou, M. Nikkhoo, M. Mehrabani, B. Amir-Heidari, A.R. Shahverdi, M. Shakibaie, *J. Trace Elem. Med Biol.* **28**, 1 (2014)
55. H. Hasim, P. Rao, A. Sekhar, S. Muthuraju, M. Asari, K. Sirajudeen, *Adv. Nat. Sci.: Nanosci. Nanotechnol.* **11**, 2 (2020)
56. A. Hosny, M. Kashef, S. Rasmy, D. Aboul-Magd, Z. El-Bazza, *Adv. Nat. Sci.: Nanosci. Nanotechnol.* **8**, 4 (2017)
57. A. Boldeiu, M. Simion, I. Mihalache, A. Radoi, M. Banu, P. Varasteanu, P. Nadejde, E. Vasile, A. Acasandrei, R.C. Popescu, *J. Photochem. Photobiol. B: Biol.* **197**, 111519 (2019)
58. E.R. Balasooriya, C.D. Jayasinghe, U.A. Jayawardena, R.W.D. Ruwanthika, R. Mendis de Silva, P.V. Udagama, *J. Nanomater.* **2017**, 1 (2017)
59. H. Haiza, A. Azizan, A.H. Mohidin, D. Halin, *Nano Hybrids* **4**, 87 (2013)
60. J. Pi, H. Jin, R. Liu, B. Song, Q. Wu, L. Liu, J. Jiang, F. Yang, H. Cai, J. Cai, *Appl. Microbiol. Biotechnol.* **97**, 3 (2013)

61. T. Nie, H. Wu, K.-H. Wong, T. Chen, J. Mater. Chem. B **4**, 13 (2016)
62. H. Zhang, Q. Sun, L. Tong, Y. Hao, T. Yu, Biomed. Pharmacother. **107**, 1135 (2018)
63. J.S. Al-Brahim, A.E. Mohammed, Saudi J. Biol. Sci. **27**, 1 (2020)
64. T.A. Qiu, M.J. Gallagher, N.V. Hudson-Smith, J. Wu, M.O. Krause, J.D. Fortner, C.L. Haynes, Environ. Sci.: Nano **3**, 5 (2016)
65. H. Wu, S. Liu, J. Gong, J. Liu, Q. Zhang, X. Leng, N. Zhang, Y. Li, Cancer Lett. **393**, 22 (2017)
66. M. Ahamed, M.J. Akhtar, M.M. Khan, H.A. Alhadlaq, A. Alshamsan, Coll. Surf. B: Biointerfaces **148**, 665 (2016)
67. K. Vasanth, K. Ilango, R. MohanKumar, A. Agrawal, G.P. Dubey, Coll. Surf. B: Biointerfaces **117**, 354 (2014)
68. H. Javid, J. Asadi, F.Z. Avval, A.R. Afshari, S.I. Hashemy, Mol. Biol. Rep. **47**, 3 (2020)
69. H. Li, D. Liu, S. Li, C. Xue, Int. J. Boil. Macromol. **129**, 818 (2019)
70. L. Ou, S. Lin, B. Song, J. Liu, R. Lai, L. Shao, Int. J. Nanomed. **12**, 6633 (2017)
71. L. Chen, L.-Y. Wu, W.-X. Yang, Nanomedicine **13**, 22 (2018)
72. S. Tummala, G. Kuppusamy, M.S. Kumar, T. Praveen, A. Wadhvani, Drug Deliv. **23**, 8 (2016)
73. Y. Li, M. Guo, Z. Lin, M. Zhao, Y. Xia, C. Wang, T. Xu, B. Zhu, R. Soc. Open Sci. **5**, 11 (2018)
74. X. Gao, X. Li, J. Mu, C.-T. Ho, J. Su, Y. Zhang, X. Lin, Z. Chen, B. Li, Y. Xie, Int. J. Biol. Macromol. **152**, 605 (2020)
75. H. Khan, M. Reale, H. Ullah, A. Sureda, S. Tejada, Y. Wang, Z.-J. Zhang, J. Xiao, Biotechnol. Adv. **38**, 107385 (2020)
76. H. Katifelis, A. Lyberopoulou, I. Mukha, N. Vityuk, G. Grodzyuk, G.E. Theodoropoulos, E.P. Efsthopoulos, M. Gazouli, Artif. Cells Nanomed. Biotechnol. **46**, 3 (2018)
77. M. Elbadawy, T. Usui, H. Yamawaki, K. Sasaki, Int. J. Mol. Sci. **20**, 9 (2019)
78. A.A. Abuderman, R. Syed, A.A. Alyousef, M.S. Alqahtani, M.S. Ola, A. Malik, Processes **7**, 11 (2019)

Publisher's Note Springer Nature remains neutral with regard to jurisdictional claims in published maps and institutional affiliations.

Authors and Affiliations

Hamed Amiri¹ · Seyed Isaac Hashemy^{1,2} · Zahra Sabouri³ · Hossein Javid⁴ · Majid Darroudi^{5,6} 

¹ Department of Clinical Biochemistry, Faculty of Medicine, Mashhad University of Medical Sciences, Mashhad, Iran

² Surgical Oncology Research Center, Mashhad University of Medical Sciences, Mashhad, Iran

³ Applied Biomedical Research Center, Mashhad University of Medical Sciences, Mashhad, Iran

⁴ Department of Medical Laboratory Sciences, Varastegan Institute for Medical Sciences, Mashhad, Iran

⁵ Nuclear Medicine Research Center, Mashhad University of Medical Sciences, Mashhad, Iran

⁶ Department of Medical Biotechnology & Nanotechnology, Faculty of Medicine, Mashhad University of Medical Sciences, Mashhad, Iran